Ain Shams Engineering Journal (2016) xxx, xxx–xxx

Ain Shams University

Ain Shams Engineering Journal

www.elsevier.com/locate/asej
www.sciencedirect.com

ENGINEERING PHYSICS AND MATHEMATICS

Study of heat and mass transport in Couple-Stress liquid under G-jitter effect

Anand Kumar [a], **Vanita** [a], **Vinod K. Gupta** [b,*]

[a] *Department of Mathematics, Central University of Rajasthan, Ajmer, India*
[b] *Department of Mathematics, DIT University, Dehradun, Uttarakhand, India*

Received 15 December 2015; revised 1 April 2016; accepted 10 May 2016

KEYWORDS

Rayleigh–Benard convection;
Couple stress liquid;
Gravity modulation;
Ginzburg–Landau equation

Abstract In the present paper, we deal with the effect of G-jitter (time periodic gravity modulation) on the stability of double diffusive convection in couple stress liquid by method of nonlinear analysis. The infinitesimal disturbances are expanded in terms of power series of amplitude of modulation. Couple stress term has been employed in momentum equation. For the stationary convection, the Ginzburg–Landau equation has been used to investigate the effect of modulation on heat and mass transfer. The effect of Prandtl number, couple stress parameter, Lewis number and solute Rayleigh number has also been investigated.

1. Introduction

The study of non-Newtonian fluids has drawn the attention of many researchers due to its physical applications in engineering techniques and industries like extraction of crude oil in petroleum industry, solidification of liquid crystals, cooling of metallic plate, exotic lubrication and colloidal and suspension solutions. In the category of non-Newtonian fluids, couple stress fluid has become the emerging field of research due to its different features, such as polar effect having large viscosity. The mechanical interactions in the fluid medium arise from the concept of couple stress. The theory of couple stress was proposed by Stokes [1] who represents the classical theory which describes the polar effect in the presence of couple stress, body couple and non-symmetric tensors.

The onset convection in a couple stress fluid saturated porous layer by using a thermal non-equilibrium model has been studied by Malashetty et al. [2]. They have studied the effect of thermal non-equilibrium on the onset of convection and showed that the results of the thermal non-equilibrium Darcy model for the Newtonian fluid case can be recovered in the limit as couple stress parameter $C \to 0$. Umavathi and Malashetty [3] investigated the oberbeck convection flow of couple stress fluid through a vertical porous spectrum. They have found that both the porous parameter and couple stress parameter suppress the flow. Shivkumara [4] analyzed the effect of non-uniform temperature gradients on the onset of convection in a couple stress fluid saturated porous medium. He made conclusion that the critical DarcyRayleigh numbers increase monotonically with an increase of couple stress parameter. Sharma and Thakur [5] carried out the thermal

* Corresponding author. Tel.: +91 9453262305.
E-mail addresses: aanandbhu@gmail.com (A. Kumar), vanitacuraj@gmail.com (Vanita), vinodguptabhu@gmail.com (V.K. Gupta).

Peer review under responsibility of Ain Shams University.

ELSEVIER Production and hosting by Elsevier

http://dx.doi.org/10.1016/j.asej.2016.05.003

Nomenclature

Latin symbols

$A(t)$	finite amplitudes of minimal representation of the Fourier series
C	couple stress parameter, $\mu_c/\mu d^2$
d	distance between plate
$\mathbf{g}$	gravitational acceleration, $(0,0,-g)$
Le	Lewis number, κ_T/κ_S
Nu	Nusselt number
p	pressure
Pr	Prandtl number, ν/κ_T
$\mathbf{q}$	velocity of the fluid (u,v,w)
Ra_T	Rayleigh number $(Ra_T = \beta_T g d(\Delta T)d^3/\nu\kappa_T)$
Ra_S	concentration Rayleigh number $(Ra_S = \beta_S g d(\Delta S)d^3/\nu\kappa_T)$
S	solute concentration
ΔS	solute difference between the walls
Sh	Sherwood number
t	time
T	temperature
ΔT	temperature difference between the walls
(x,z)	co-ordinate axis

Greek symbols

β_T	thermal expansion coefficient
β_S	concentration expansion coefficient
δ_1	amplitude of modulation
ϵ	expansion parameter
k_c	Wave number
κ_T	thermal diffusivity
κ_S	solute diffusivity
μ	dynamic viscosity
μ_c	couple stress viscosity
ν	kinematic viscosity, μ/ρ_0
Ω	frequency of modulation
ψ	stream function
ρ	density
ρ_0	density at reference temperature
τ	slow timescale
σ	growth rate

Other symbols

b	basic state
c	critical
$*$	non-dimensional term
st	stationary

stability of an electrically conducting Couple-Stress fluid saturated porous layer in the presence of magnetic field and found that the couple stress parameter delays the onset of stationary convection while Sharma and Sharma [6] investigated the onset of convection in a couple stress fluid saturated porous layer in the presence of rotation and magnetic field and found that the magnetic field and rotation have stabilizing effects on stationary convection.

The double diffusive convection is of considerable importance in various fields such as high quality crystal production, liquid gas storage, oceanography, production of pure medication, solidification of molten alloys and geothermally heated lakes and magmas. Nield [7] studied the onset of thermohaline convection in a porous medium and concluded that oscillatory instability may be possible when a strongly stabilizing solute gradient is opposed by a destabilizing thermal gradient. Malashetty et al. [8] presented an analytical study of linear and nonlinear double diffusive convection with Soret effect in couple stress liquids and found that the effect of couple stress is quite large. Malashetty and Kollur [9] discussed the onset of double diffusive convection in a couple stress fluid saturated anisotropic porous layer. They reported that the thermal anisotropy parameter, couple stress parameter, and solute Rayleigh number have stabilizing effect on the stationary, oscillatory, and finite amplitude convection.

The linear stability analysis of Rayleigh–Benard convection for the small amplitude temperature modulation was firstly discussed by Venezian [10]. Later on, several studies have been made by Rosenblat and Herbert [11], Rosenblat and Tanaka [12], Roppo et al. [13], Bhadauria and Bhatia [14], Siddheshwar and Abraham [15], Bhadauria [16] Malashetty et al. [17], Bhadauria and Debnath [18] and Bhadauria et al. [30].

The effect of gravity modulation on convective stable configuration can significantly influence the stability of a system by increasing or decreasing its susceptibility to convection. Grasho and Sani [19] investigated the effect of gravity modulation on the stability of a heated fluid layer and found that the gravity modulation can significantly affect the stability limits of the system. Wadih and Roux [20] studied the effect of small amplitude gravity modulation on convection in long cylindrical cavities. Malashetty and Begum [21] investigated the effect of thermal/gravity modulation on the onset of convection in a Maxwell Fluid saturated porous layer by linear stability analysis and gave results that the low frequency symmetric thermal modulation is destabilizing while moderate and high frequency symmetric modulation is stabilizing. Also, Kumar and Bhadauria [22] have carried out the thermal instability in a rotating anisotropic porous layer saturated by a viscoelastic fluid and draw conclusion that the rotation inhibits the onset of convection in both stationary and oscillatory modes. Bhadauria et al. [23] have studied the gravity modulation in a fluid layer. They performed the stability analysis which tells us about the criteria for the onset of convection (i.e. the Rayleigh number) only and does not provide any information about the heat and mass transfer. Gupta and Singh [24] investigated the double diffusive reaction convection in viscous fluid layer. Further, Gupta and Singh [25] and Gupta et al. [26] have done studies on chaos.

Ginzburg–Landau equations arise as a solvability condition in a wide variety of problems in continuum mechanics while dealing with a weakly non-linear stability analysis, e.g. one can deal Ginzburg–Landau equations with constant and real coefficient in the case of Rayleigh–Benard convection in fluids where instability sets as a direct mode (also called stationary mode). There are in-homogeneous GL equations also. Bhaduria et al. [27] analyzed the effect of thermal/gravity modulation in a rotating fluid saturated porous layer by performing non-linear stability using Ginburg–Landau equations.

Please cite this article in press as: Kumar A et al., Study of heat and mass transport in Couple-Stress liquid under G-jitter effect, Ain Shams Eng J (2016), http://dx.doi.org/10.1016/j.asej.2016.05.003

Srivastava et al. [28] and Gupta and Bhadauria [29] have done studies on double diffusion with soret effect.

In this study the Ginzburg–Landau equation for stationary mode of G-jitter (which is also known as time periodic gravity modulation) natural convection in a couple stress fluid has been investigated. The Ginzburg–Landau equation has been solved numerically and consequently the effect of modulation on the heat transfer coefficient-Nusselt number and Mass transfer coefficient-Sherwood number has been studied. A detailed discussion has been given which tells us importance of this investigation.

2. Mathematical formulation

Consider the double diffusive convection in couple stress fluid saturated porous layer, confined between two parallel infinite horizontal plates $z = 0$ and $z = d$ at a distance d apart. The fluid layer is heated from below and cooled from above to maintain a constant gradient temperature $\triangle T$ across the layer. We have chosen a Cartesian frame of reference in which the origin lies on the lower plate and the z-axis vertically upwards (see Fig. 1). According to consideration, the governing equations of the model for the motion of an incompressible couple stress fluid in the absence of body couple are obtained as follows (Malashetty and Kollur [9], Gupta and Singh [24] and Bhadauria et al. [27]):

$$\nabla \cdot \mathbf{q} = 0, \tag{1}$$

$$\rho_0\left[\frac{\partial \mathbf{q}}{\partial t} + (\mathbf{q}\cdot\nabla)\mathbf{q}\right] = -\nabla \mathbf{p} + \rho \mathbf{g} + (\mu - \mu_c\nabla^2)\nabla^2\mathbf{q}, \tag{2}$$

where $\mathbf{g} = (0, 0, -g)$ and $g = g_0[1 + \varepsilon^2\delta_1 \cos(\Omega t)]$

where $\mathbf{g}$ denotes the acceleration due to the gravity and g_0 is some reference value of the gravitational force, Ω is the frequency of modulation. The quantity $\epsilon^2\delta_1$ is the amplitude of modulation, where ϵ and δ_1 both are small, resulting the modulation to be of small amplitude.

The energy, mass diffusion and basic state equations are as follows:

$$\frac{\partial T}{\partial t} + (\mathbf{q}\cdot\nabla)T = \kappa_T\nabla^2 T, \tag{3}$$

$$\frac{\partial S}{\partial t} + (\mathbf{q}\cdot\nabla)S = \kappa_S\nabla^2 S, \tag{4}$$

$$\rho = \rho_0[1 - \beta_T(T - T_0) + \beta_S(S - S_0)]. \tag{5}$$

The boundary conditions for temperature and mass transfer are given by

$$\begin{aligned} &T = T_0 + \Delta T \quad \text{and} \quad S = S_0 + \Delta S \text{ at } z = 0,\\ &T = T_0 \quad \text{and} \quad S = S_0 \text{ at } z = d, \end{aligned} \tag{6}$$

where $\mathbf{q}$ is the velocity, ρ_0 represents the density at the reference temperature T_0 (temperature of the upper plate), p the pressure, ρ the density, μ the dynamic coefficient of viscosity, μ_c the couple stress viscosity, T the temperature, S is the solute concentration. Further, κ_T is the thermal diffusivity, κ_S is the solute diffusivity of the liquid, β_T is the coefficient of thermal expansion and β_S is the coefficient of solute expansion.

The basic state is assumed to be quiescent, i.e.,

$$q_b = 0; \quad \rho = \rho_b(z); \quad p = p_b(z); \quad T = T_b(z); \quad S = S_b(z),$$

which satisfy the following equations:

$$\frac{dp_b}{dz} = -\rho_b \mathbf{g}, \tag{7}$$

$$\frac{d^2T_b}{dz^2} = 0, \tag{8}$$

$$\frac{d^2S_b}{dz^2} = 0. \tag{9}$$

Solution of Eqs. (8) and (9) using the boundary conditions (6) are given by

$$T_b = T_0 + \Delta T\left(1 - \frac{z}{d}\right), \tag{10}$$

$$S_b = S_0 + \Delta S\left(1 - \frac{z}{d}\right). \tag{11}$$

Eliminating pressure term from Eq. (2) by taking curl on both sides and introducing stream function $u = \frac{\partial \psi}{\partial z}$, and $w = -\frac{\partial \psi}{\partial x}$, we get

$$\rho_0\left[\frac{\partial}{\partial t}(\nabla^2\psi) - \frac{\partial(\psi, \nabla^2\psi)}{\partial(x,z)}\right] = \mu\nabla^4\psi - \mu_c\nabla^6\psi + \beta_T\mathbf{g}\frac{\partial T}{\partial x} - \beta_S\mathbf{g}\frac{\partial S}{\partial x}. \tag{12}$$

Now consider infinitesimal perturbations to the basic state solution in the form of

$$\psi = \psi_b + \psi', \quad T = T_b + T', \quad \rho = \rho_b + \rho', \quad S = S_b + S'.$$

Substituting the above parameters in Eqs. (12), (3) and (4), we get the following equations:

$$\rho_0\left[\frac{\partial}{\partial t}(\nabla^2\psi') - \frac{\partial(\psi', \nabla^2\psi')}{\partial(x,z)}\right] = \mu\nabla^4\psi' - \mu_c\nabla^6\psi' + \beta_T\vec{g}\frac{\partial T'}{\partial x} - \beta_S\vec{g}\frac{\partial S'}{\partial x}, \tag{13}$$

$$\frac{\partial T'}{\partial t} - \frac{\partial(\psi', T')}{\partial(x,z)} = \kappa_T\nabla^2 T' - \frac{\partial \psi'}{\partial x}\frac{\Delta T'}{d}, \tag{14}$$

$$\frac{\partial S'}{\partial t} - \frac{\partial(\psi', S')}{\partial(x,z)} = \kappa_S\nabla^2 S' - \frac{\partial \psi'}{\partial x}\frac{\Delta S'}{d}. \tag{15}$$

The Eqs. (13)–(15) are rendered dimensionless using the following transformations:

$$\psi' = \kappa_T\psi^*, \quad (x,z) = d(x^*, z^*), \quad t = \frac{d^2}{\kappa_T}t^*, \quad T' = (\Delta T)T^*,$$

$$S' = (\triangle S')S^*, \quad \omega = \frac{\Omega}{\epsilon^2}.$$

The Eqs. (13)–(15) in dimensionless form are obtained as follows:

$$C\nabla^6\psi^* - \nabla^4\psi^* - \frac{1}{Pr}\frac{\partial(\psi^*, \nabla^2\psi^*)}{\partial(x^*, z^*)} = -\frac{1}{Pr}\frac{\partial}{\partial t^*}(\nabla^2\psi^*) - (1 + \epsilon^2\delta_1 cos\Omega t^*)\left(Ra_T\frac{\partial T^*}{\partial x^*} - Ra_S\frac{\partial S^*}{\partial x^*}\right), \tag{16}$$

$$-\nabla^2 T^* + \frac{\partial \psi^*}{\partial x^*} = -\frac{\partial T^*}{\partial t^*} + \frac{\partial(\psi^*, T^*)}{\partial(x^*, z^*)}, \tag{17}$$

$$\frac{\partial \psi^*}{\partial x^*} - \frac{1}{Le}\nabla^2 S^* = -\frac{\partial S^*}{\partial t^*} + \frac{\partial(\psi^*, S^*)}{\partial(x^*, z^*)}, \tag{18}$$

where asterisks denote the dimensionless values. $Pr = \frac{\nu}{\kappa_T}$ represents the Prandtl number, $Ra_S = \frac{\beta_S g \Delta T d^3}{\nu \kappa_T}$, the solute Rayleigh number, $Ra_T = \frac{\beta_T g \Delta T d^3}{\nu \kappa_T}$, the Rayleigh number, $C = \frac{\mu_c}{\mu d^2}$, the couple stress parameter and $Le = \frac{\kappa_T}{\kappa_S}$, the Lewis number.

The boundary conditions for the perturbed state are given by,

$$\psi^* = \nabla^2\psi^* = T^* = 0 \quad \text{at } z^* = 0, 1. \tag{19}$$

After dropping the asterisks we can write the above equations as,

$$(C\nabla^2 - 1)\nabla^4\psi + (1 + \epsilon^2\delta_1 \cos \Omega t)\left(Ra_T \frac{\partial T}{\partial x} - Ra_S \frac{\partial S}{\partial x}\right) = -\frac{1}{Pr}\frac{\partial}{\partial t}(\nabla^2\psi) - \frac{1}{Pr}\frac{\partial(\psi, \nabla^2\psi)}{\partial(x, z)}, \tag{20}$$

$$\frac{\partial \psi}{\partial x} - \nabla^2 T = -\frac{\partial T}{\partial t} + \frac{\partial(\psi, T)}{\partial(x, z)}, \tag{21}$$

$$\frac{\partial \psi}{\partial x} - \frac{1}{Le}\nabla^2 S = -\frac{\partial S}{\partial t} + \frac{\partial(\psi, S)}{\partial(x, z)}. \tag{22}$$

3. Non-linear stability analysis

We will use the time variations only at the slow timescale $\tau = \epsilon^2 t$

$$\begin{bmatrix} -\nabla^4 + C\nabla^6 & [1 + \epsilon^2\delta_1 \cos(\omega\tau)]Ra_T \frac{\partial}{\partial x} & -Ra_S[1 + \epsilon^2\delta_1 \cos(\omega\tau)]\frac{\partial}{\partial x} \\ \frac{\partial}{\partial x} & -\nabla^2 & 0 \\ \frac{\partial}{\partial x} & 0 & -\frac{1}{Le}\nabla^2 \end{bmatrix} \times \begin{bmatrix} \psi \\ T \\ S \end{bmatrix} = \begin{bmatrix} -\frac{\epsilon^2}{Pr}\frac{\partial}{\partial \tau}(\nabla^2\psi) + \frac{1}{Pr}\frac{\partial(\psi, \nabla^2\psi)}{\partial(x,z)} \\ -\epsilon^2 \frac{\partial T}{\partial \tau} + \frac{\partial(\psi, T)}{\partial(x,z)} \\ -\epsilon^2 \frac{\partial S}{\partial \tau} + \frac{\partial(\psi, S)}{\partial(x,z)} \end{bmatrix}. \tag{23}$$

Now we use the following perturbations in Eq. (23):

$$\left.\begin{aligned} Ra_T &= Ra_{T_0} + \epsilon^2\, Ra_{T_2} + \cdots \\ \psi &= \epsilon\, \psi_1 + \epsilon^2\, \psi_2 + \cdots \\ T &= \epsilon\, T_1 + \epsilon^2\, T_2 + \cdots \\ S &= \epsilon\, S_1 + \epsilon^2\, S_2 + \cdots \end{aligned}\right\}, \tag{24}$$

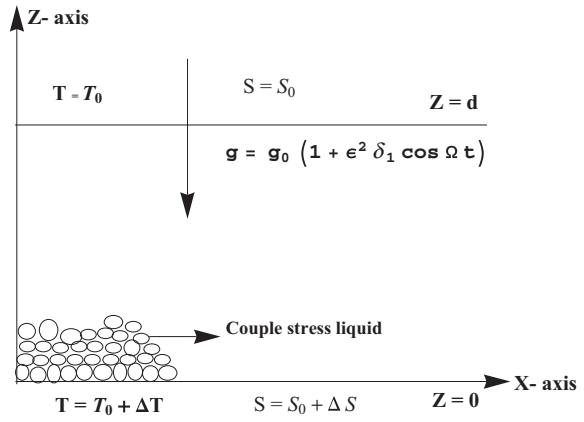

Figure 1 Schematic diagram of problem formulation.

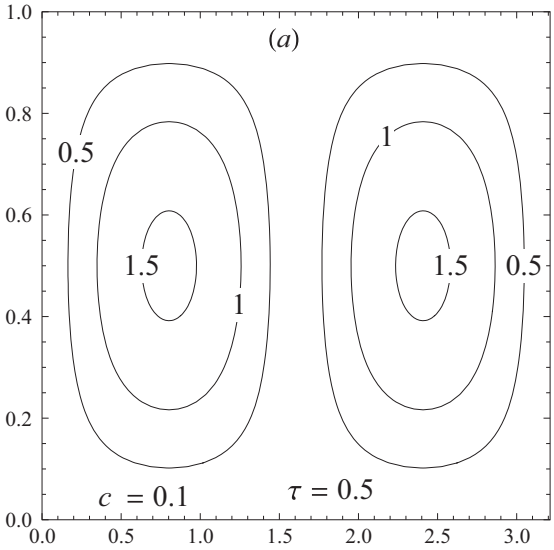

Figure 2 Streamlines for $Pr = 0.6$, $Le = 2$, $Ra_S = 50$, $\omega = 2$, $\delta_1 = 0.05, \tau = 0.5$ and $C = 0.1$.

where Ra_{T_0} is the critical Rayleigh number at which convection sets without modulation, ϵ is the expansion parameter and subscripts are the series representation of perturbation. Substituting Eq. (24) in (23) and comparing like powers of ϵ on both sides, we get solutions of different orders:

Solution for the first order case,

$$\begin{bmatrix} -\nabla^4 + C\nabla^6 & Ra_{T_0}\frac{\partial}{\partial x} & -Ra_S\frac{\partial}{\partial x} \\ \frac{\partial}{\partial x} & -\nabla^2 & 0 \\ \frac{\partial}{\partial x} & 0 & -\frac{1}{Le}\nabla^2 \end{bmatrix} \begin{bmatrix} \psi_1 \\ T_1 \\ S_1 \end{bmatrix} = \begin{bmatrix} 0 \\ 0 \\ 0 \end{bmatrix}. \tag{25}$$

The solutions of the above equations can be written as,

$$\left.\begin{aligned} \psi_1 &= A(\tau)\sin(k_c x)\sin(\pi z) \\ T_1 &= -\tfrac{k_c}{\delta^2} A(\tau)\cos(k_c x)\sin(\pi z) \\ S_1 &= -\tfrac{k_c Le}{\delta^2} A(\tau)\cos(k_c x)\sin(\pi z) \end{aligned}\right\}, \tag{26}$$

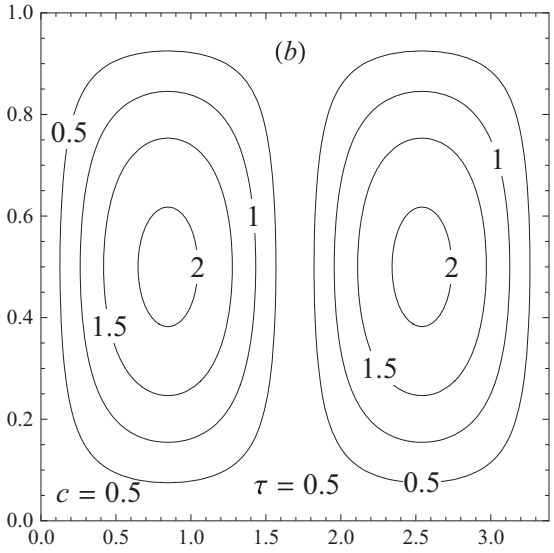

Figure 3 Streamlines for $Pr = 0.6$, $Le = 2$, $Ra_S = 50$, $\omega = 2$, $\delta_1 = 0.05$, $\tau = 0.5$ and $C = 0.5$.

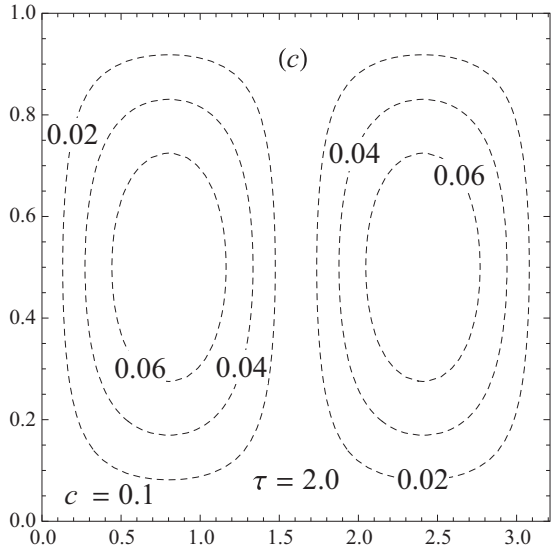

Figure 4 Streamlines for $Pr = 0.6$, $Le = 2$, $Ra_S = 50$, $\omega = 2$, $\delta_1 = 0.05, \tau = 2.0$ and $C = 0.1$.

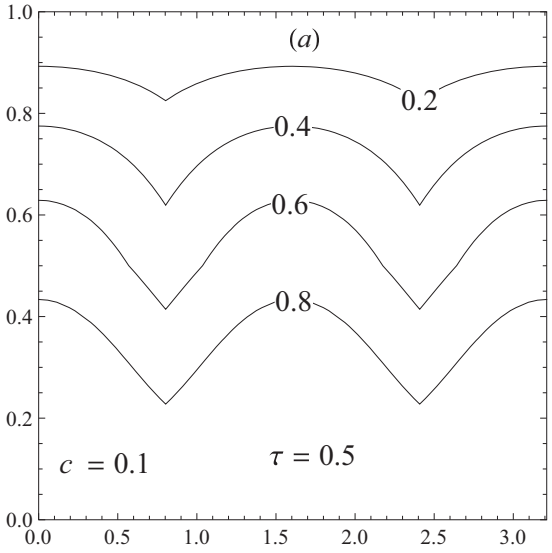

Figure 6 Isotherms for $Pr = 0.6$, $Le = 2$, $Ra_S = 50$, $\omega = 2$, $\delta_1 = 0.05$, $\tau = 0.5$ and $C = 0.1$.

where ψ_1, T_1 and S_1 are the first solution of perturbation series, $A(\tau)$ is the finite amplitude of minimal representation of Fourier series, k_c is the wave number, and δ is the modulation amplitude. The system (25) gives us the critical Rayleigh number as follows:

$$Ra_{T_0} = Ra_S Le + \frac{\delta^6}{k_c^2} + C\frac{\delta^8}{k_c^2}. \tag{27}$$

4. Amplitude equation (Ginzburg–Landau equation): heat and mass transport for stationary instability

Solution for the second order case is

$$\begin{bmatrix} -\nabla^4 + C\nabla^6 & Ra_{T_0}\frac{\partial}{\partial x} & -Ra_S\frac{\partial}{\partial x} \\ \frac{\partial}{\partial x} & -\nabla^2 & 0 \\ \frac{\partial}{\partial x} & 0 & -\frac{1}{Le}\nabla^2 \end{bmatrix} \begin{bmatrix} \psi_2 \\ T_2 \\ S_2 \end{bmatrix} = \begin{bmatrix} \Re_{21} \\ \Re_{22} \\ \Re_{23} \end{bmatrix}, \tag{28}$$

where,

$$\Re_{21} = \frac{1}{Pr}\frac{\partial(\psi_1, \nabla^2\psi_1)}{\partial(x,z)} = 0, \tag{29}$$

$$\Re_{22} = \frac{\partial(\psi_1, T_1)}{\partial(x,z)} = -\frac{k_c^2\pi}{2\delta^2}[A(\tau)]^2 \sin(2\pi z), \tag{30}$$

$$\Re_{23} = \frac{\partial(\psi_1, S_1)}{\partial(x,z)} = -\frac{k_c^2\pi Le}{2\delta^2}[A(\tau)]^2 \sin(2\pi z), \tag{31}$$

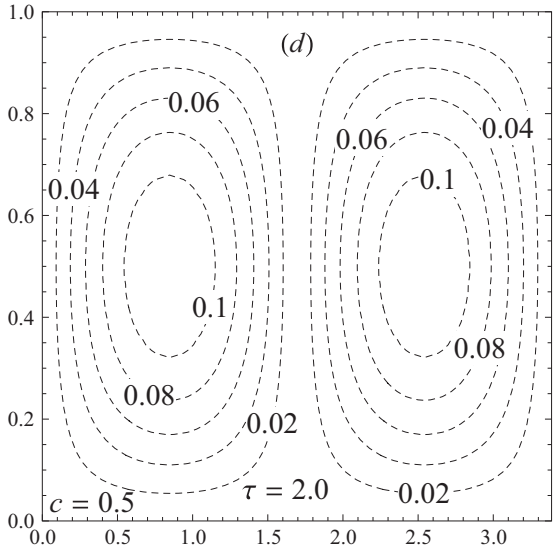

Figure 5 Streamlines for $Pr = 0.6$, $Le = 2$, $Ra_S = 50$, $\omega = 2$, $\delta_1 = 0.05, \tau = 2.0$ and $C = 0.5$.

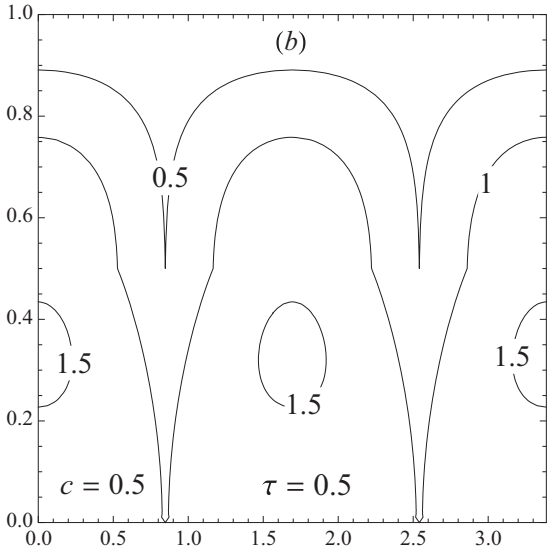

Figure 7 Isotherms for $Pr = 0.6$, $Le = 2$, $Ra_S = 50$, $\omega = 2$, $\delta_1 = 0.05$, $\tau = 0.5$ and $C = 0.5$.

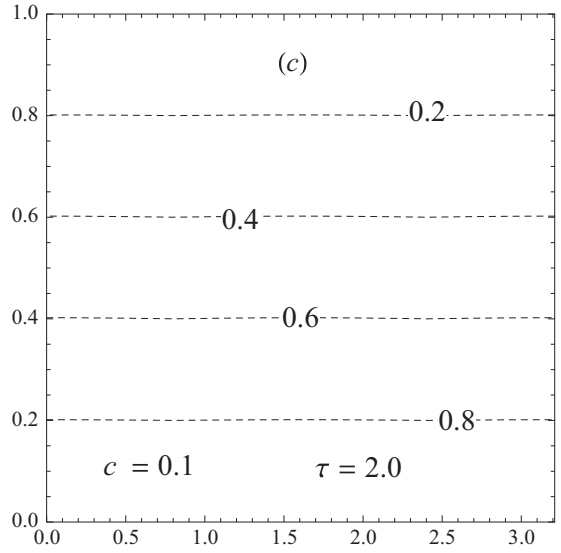

Figure 8 Isotherms for $Pr = 0.6$, $Le = 2$, $Ra_S = 50$, $\omega = 2$, $\delta_1 = 0.05, \tau = 2.0$ and $C = 0.1$.

We can obtain second order solution as,

$$\left.\begin{aligned} \psi_2 &= 0, \\ T_2 &= -\tfrac{k_c^2}{8\pi\delta^2}[A(\tau)]^2 \sin(2\pi z), \\ S_2 &= -\tfrac{k_c^2 Le}{8\pi\delta^2}[A(\tau)]^2 \sin(2\pi z). \end{aligned}\right\} \tag{32}$$

Solution for the third order case is

$$\begin{bmatrix} -\nabla^4 + C\nabla^6 & Ra_{T_0}\frac{\partial}{\partial x} & -Ra_S\frac{\partial}{\partial x} \\ \frac{\partial}{\partial x} & -\nabla^2 & 0 \\ \frac{\partial}{\partial x} & 0 & -\frac{1}{Le}\nabla^2 \end{bmatrix} \begin{bmatrix} \psi_3 \\ T_3 \\ S_3 \end{bmatrix} = \begin{bmatrix} \Re_{31} \\ \Re_{32} \\ \Re_{33} \end{bmatrix}, \tag{33}$$

where

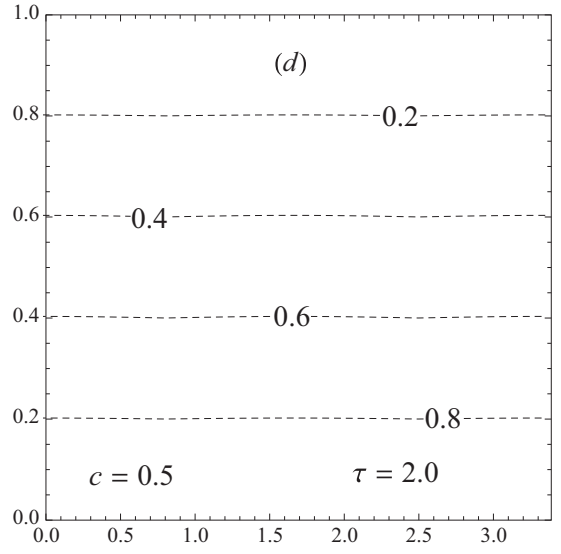

Figure 9 Isotherms for $Pr = 0.6$, $Le = 2$, $Ra_S = 50$, $\omega = 2$, $\delta_1 = 0.05, \tau = 2.0$ and $C = 0.5$.

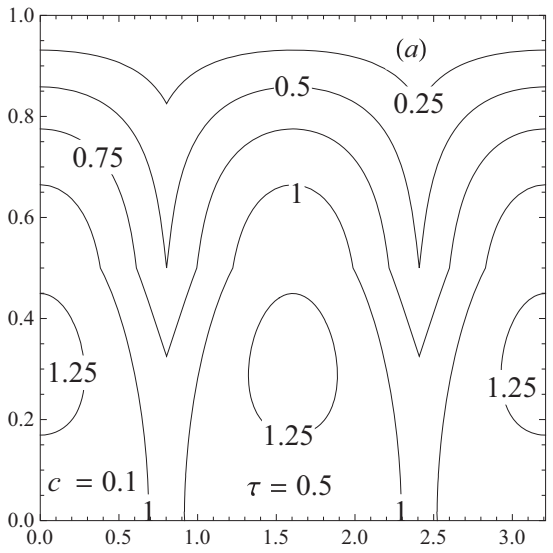

Figure 10 Isohalines for $Pr = 0.6$, $Le = 2$, $Ra_S = 50$, $\omega = 2$, $\delta_1 = 0.05, \tau = 0.2$ and $C = 0.1$.

$$\Re_{31} = -[Ra_{T_2} + Ra_{T_0}\delta_1 \cos(\omega\tau)]\frac{\partial T_1}{\partial x} - \frac{1}{Pr}\frac{\partial}{\partial \tau}(\nabla^2\psi_1) + Ra_S\delta_1 \cos(\omega\tau)\frac{\partial S_1}{\partial x}, \tag{34}$$

$$\Re_{32} = \frac{\partial \psi_1}{\partial x}\frac{\partial T_2}{\partial z} - \frac{\partial T_1}{\partial \tau}, \tag{35}$$

$$\Re_{33} = \frac{\partial \psi_1}{\partial x}\frac{\partial S_2}{\partial z} - \frac{\partial S_1}{\partial \tau}. \tag{36}$$

The solvability condition for the third order solution is given by,

$$\int_{z=0}^{1}\int_{x=0}^{\frac{2\pi}{k_c}} \left[\hat{\psi}_1\Re_{31} + Ra_{T_0}\widehat{T}_1\Re_{32} - Ra_S\widehat{S}_1\Re_{33}\right] dx\,dz = 0, \tag{37}$$

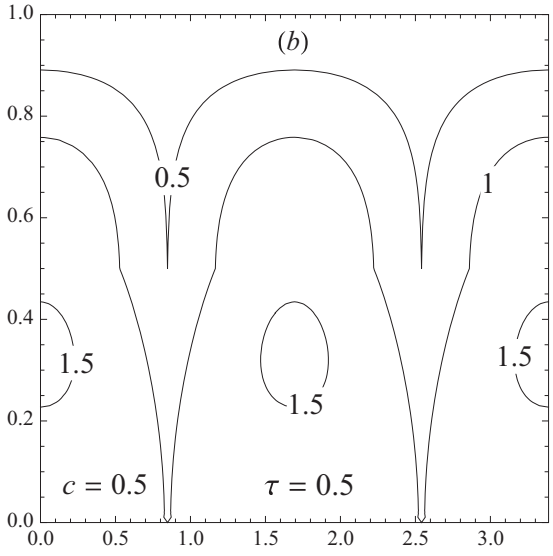

Figure 11 Isohalines for $Pr = 0.6$, $Le = 2$, $Ra_S = 50$, $\omega = 2$, $\delta_1 = 0.05, \tau = 0.5$ and $C = 0.5$.

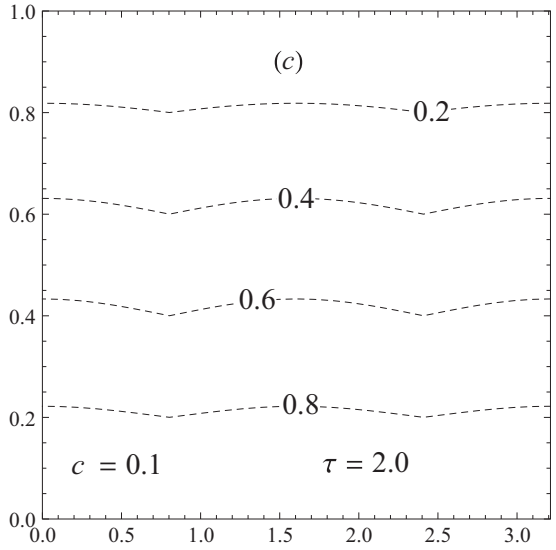

Figure 12 Isohalines for $Pr = 0.6$, $Le = 2$, $Ra_S = 50$, $\omega = 2$, $\delta_1 = 0.05, \tau = 2.0$ and $C = 0.1$.

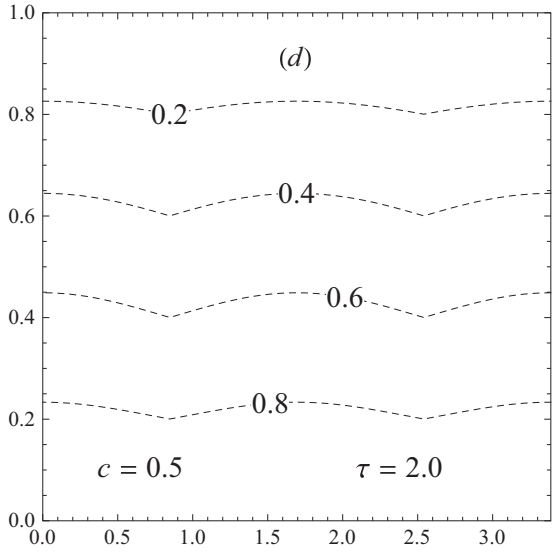

Figure 13 Isohalines for $Pr = 0.6$, $Le = 2$, $Ra_S = 50$, $\omega = 2$, $\delta_1 = 0.05, \tau = 2.0$ and $C = 0.5$.

$$\left.\begin{aligned}\hat{\psi}_1 &= -A(\tau)\sin(k_c x)\sin(\pi z)\\ \widehat{T}_1 &= -\tfrac{k_c}{\delta^2}A(\tau)\cos(k_c x)\sin(\pi z)\\ \widehat{S}_1 &= -\tfrac{k_c Le}{\delta^2}A(\tau)\cos(k_c x)\sin(\pi z)\end{aligned}\right\}. \tag{38}$$

Now substituting Eqs. (34)–(36) and Eq. (38) into the Eq. (37) and solving the integration, we get the Ginzburg–Landau equation for stationary instability with a time-periodic coefficient in the form of

$$\left[\frac{\delta^2}{Pr} + Ra_{T_0}\frac{k_c^2}{\delta^4} - Ra_S Le^2\frac{k_c^2}{\delta^4}\right]\frac{dA}{d\tau} - f(\tau)A(\tau) + \frac{k_c^2}{8\delta^4}\left[Ra_{T_0} - Le^3 Ra_S\right]A^3(\tau) = 0, \tag{39}$$

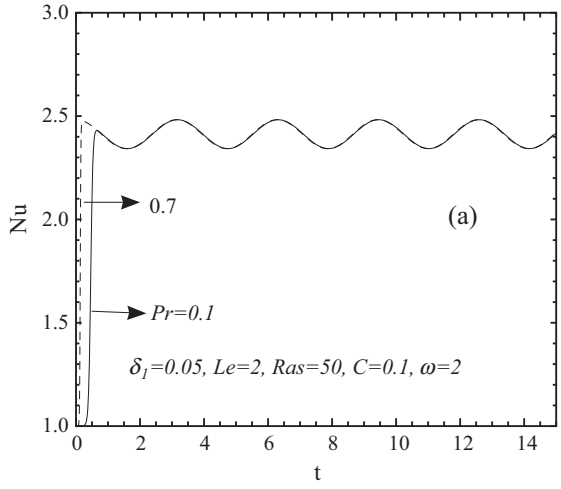

Figure 14 Variation of Nusselt number Nu with time τ for different values of Pr.

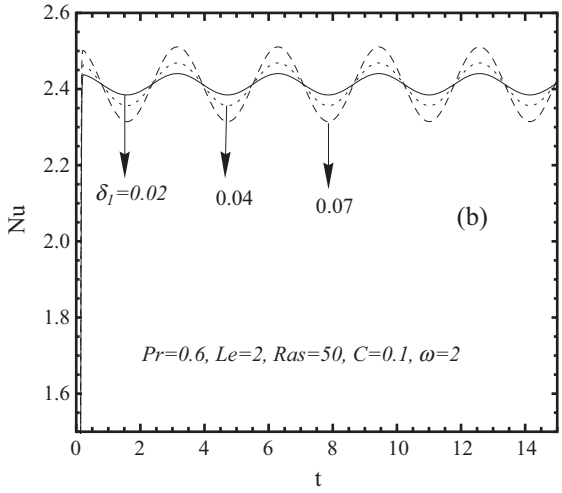

Figure 15 Variation of Nusselt number Nu with time τ for different values of δ_1.

where

$$f(\tau) = \frac{k_c^2}{\delta^2}\left[Ra_{T_2} + (Ra_{T_0} - LeRa_S)\delta_1\cos(\omega\tau)\right]. \tag{40}$$

The solution of Eq. (39), subject to the initial condition $A(0) = a_0$, where a_0 is a chosen initial amplitude of convection, can be solved by using Runge–Kutta method. We assume that $Ra_{T_2} = Ra_{T_0}$ to keep the parameters to minimum.

In particular, the Nusselt number ($Nu(\tau)$) and Sherwood number ($Sh(\tau)$) for stationary convection can be obtained as,

$$Nu(\tau) = 1 + \frac{k_c^2[A(\tau)]^2}{4\delta^2}, \tag{41}$$

$$Sh(\tau) = 1 + \frac{k_c^2 Le^2[A(\tau)]^2}{4\delta^2}. \tag{42}$$

5. Result and discussions

In the present paper, we have studied heat and mass transport in Couple-Stress liquid under G-jitter effect and presented the results graphically.

Figs. 2–5 present the graphs of streamlines for different values of time $\tau = 0.5, 2.0$ and $C = 0.1, 0.5$, by keeping other parameters constant as $Pr = 0.6, \omega = 2, Le = 2, Ra_S = 50$ and $\delta_1 = 0.05$. In Fig. 2, we have presented the graphs for streamlines by taking value of time $\tau = 0.5$ and by keeping $C = 0.1$. From the Fig. 2 we observed that stream lines are elliptic closed curves for all values τ and C which show that convection is in progress. Also, the magnitude of stream function decreases from hot wall to cold wall. Fig. 3, represents the sketches for streamlines for time $\tau = 0.5$ and $C = 0.5$ and it reveals that the influence of the parameters on the counters size comes about only after some initial time. Figs. 4 and 5 delineate graphs of stream lines for values of $C = 0.1$ and 0.5 respectively by keeping $\tau = 2.0$ fixed. From these Figs. 2–5 it is analyzed that the convection process becomes rapid with increase in value of C. From the comparative study of Figs. 3 and 5 we observed that magnitude of stream function decreases with increase in value of time τ. Thus the parameter C increases the convection and at high value of τ convection converted to conduction which can be seen by the isotherms, Figs. 2–5.

Fig. 6 depicts sketches for isotherms for $\tau = 0.5$ and $C = 0.1$. From Fig. 6, we examined that near the boundaries the isotherms are flat which show slow convection and in the middle they become counter like indicating increase in convection. In Fig. 7 we draw sketches for isotherms $\tau = 0.5$ and $C = 0.5$. We observed that on increasing value of C, the process of convection becomes rapid. Fig. 8 shows graphs of isotherms for $\tau = 2.0$ and $C = 0.1$. Here, isotherms are straight lines which indicate conduction mode. In Fig. 9 the results obtained are qualitatively similar to that obtained for Fig. 8. Figs. 10–13 represent graphs for isohalines for different values of τ and C. Fig. 10 reveals that conduction is converting into convection. We obtained the qualitatively similar results from Fig. 11 as in Fig. 10. The value of isohalines increases with increase in value of C. Figs. 12 and 13 show isohalines for values of $C = 0.1$ and $C = 0.5$ respectively by taking $\tau = 2$. These Figs. 12 and 13 indicate the conduction mode.

In Fig. 14, we have presented the variations of Nu profile with respect to slow time for different values of Prandtl number by keeping other parameters constant. From Fig. 14, it can be depicted that initially, Nu profiles increase with increases in Prandtl number but as the time passes the effect becomes negligible and the profile becomes oscillatory. Fig. 15 shows the variation of Nu profiles with respect to slow time for different values of amplitude of modulation δ_1. Fig. 15 depicts that on increasing the value of δ_1, value of Nu increases which results in increase in convection; however, the wavelength of oscillations remains unchanged. In Fig. 16, influence of Le on Nu profiles has been shown by keeping other parameters constant. It is clear from Fig. 16 that influence of Le is to increase the Nu profile which describes that the effect of this parameters is to advance the heat transfer rate. Fig. 17, presents the effect of Ra_S on Nu profile with respect to slow time. It can be clearly noticed that the effect is qualitatively similar to that obtained in Fig. 16. Fig. 18, delineates the effect of couple

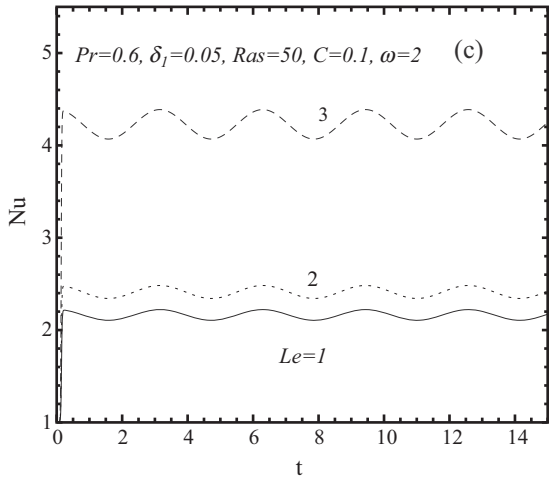

Figure 16 Variation of Nusselt number Nu with time τ for different values of Le.

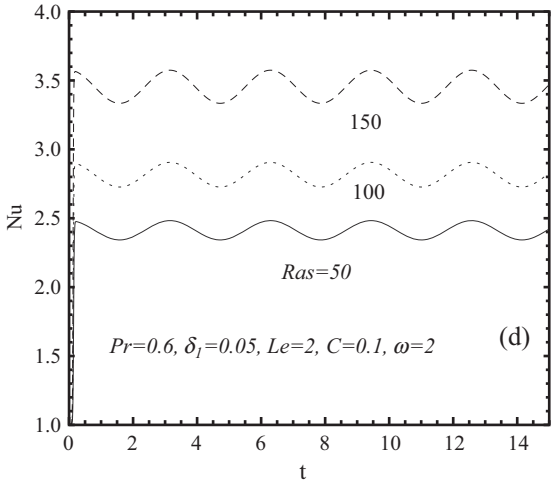

Figure 17 Variation of Nusselt number Nu with time τ for different values of Ra_S.

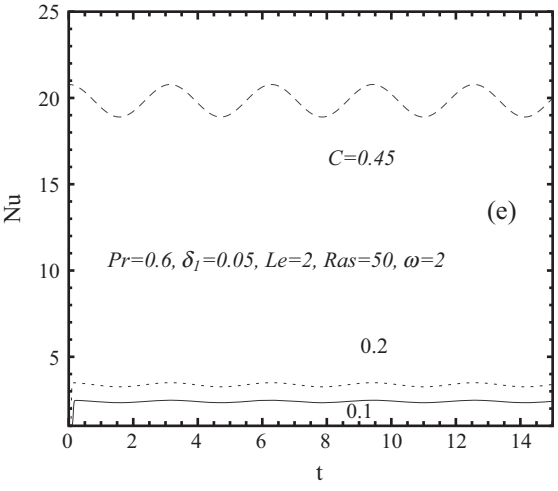

Figure 18 Variation of Nusselt number Nu with time τ for different values of C.

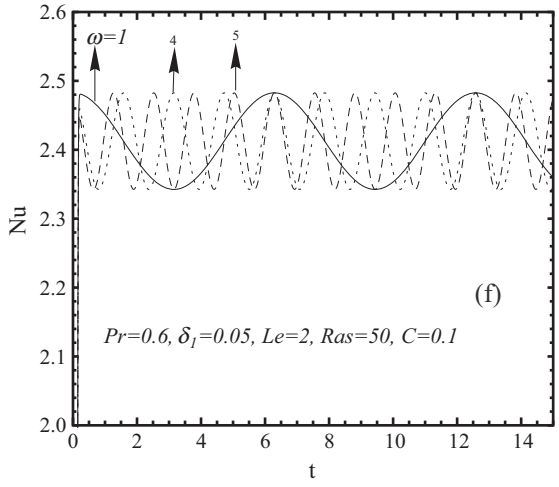

Figure 19 Variation of Nusselt number Nu with time τ for different values of ω.

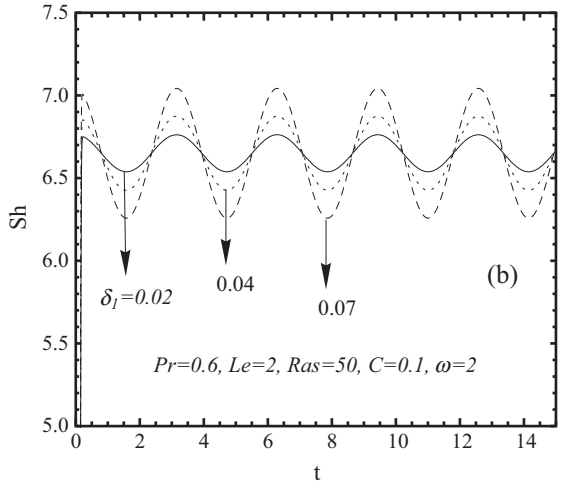

Figure 21 Variation of Sherwood number Sh with time τ for different values of δ_1.

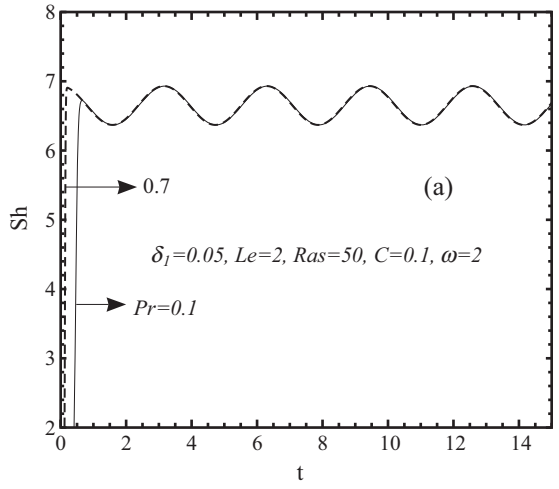

Figure 20 Variation of Sherwood number Sh with time τ for different values of Pr.

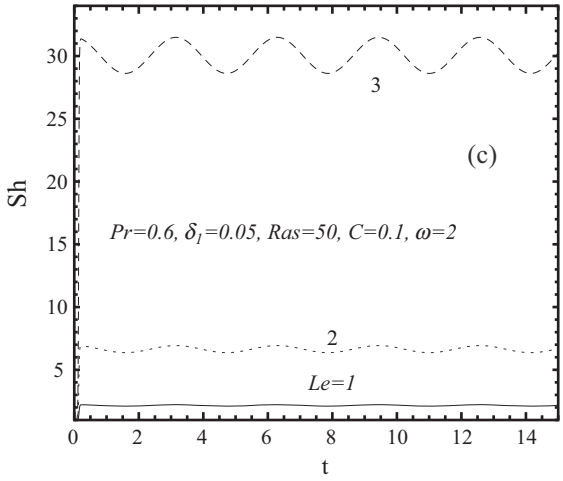

Figure 22 Variation of Sherwood number Sh with time τ for different values of Le.

stress parameter C on Nu profile with respect to slow time. It is revealed that on increasing the value of C, the value of Nusselt number also increases. It is also observed that for low values of C the profiles are unmodulated but for higher values of C the profiles become oscillatory which indicate convection mode. Fig. 19 depicts the effect of frequency of modulation ω on Nu profile. From Fig. 19 we observed that on increasing ω, the value of Nu remains unaltered whereas the wavelength of oscillations decreases.

Fig. 20 represents the variations of Sh profile for different values of Pr by keeping other parameters constant. It can be observed that the influence of Pr is to increase the Sh profiles but when time increases the effect of Pr becomes negligible and the profile becomes oscillatory. Fig. 21 shows the variation of Sh profile for different values of δ_1. From Fig. 21, we observed that with increase in amplitude of modulation δ_1, the value of Sh increases; however, the wavelength of oscillations remains unchanged. Fig. 22 depicts the effect of Le on Sh profile by keeping other parameters constant. From Fig. 22, we reveal

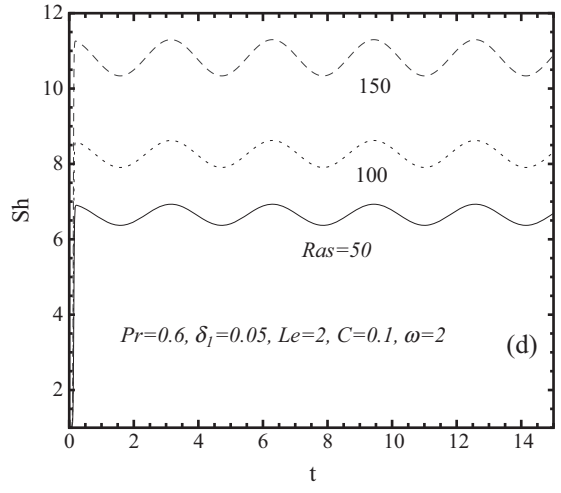

Figure 23 Variation of Sherwood number Sh with time τ for different values of Ra_S.

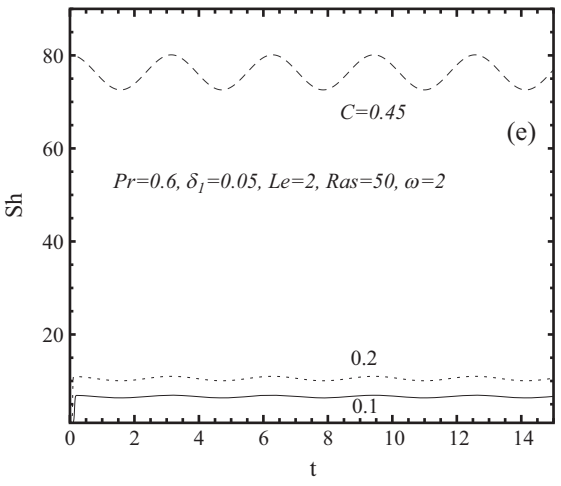

Figure 24 Variation of Sherwood number Sh with time τ for different values of C.

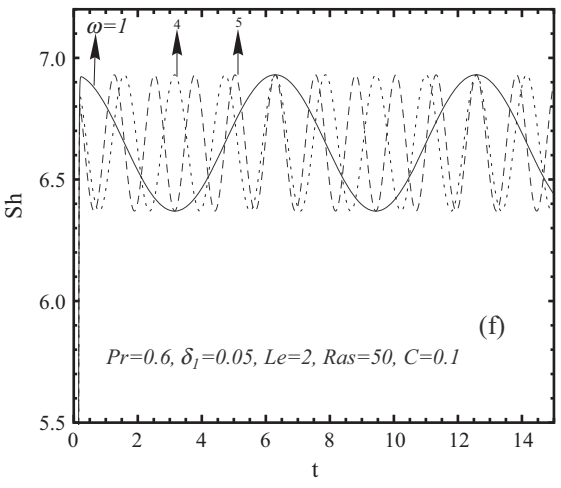

Figure 25 Variation of Sherwood number Sh with time τ for different values of ω.

that the influence of increasing Le is to increase the value of Sh which clearly indicates that the effect of this parameters is to advance the mass transfer rate. Fig. 23 represents the effect of Ra_S on Sh profile. It is clear from Fig. 23 that the effect of Ra_S is to increase the Sh profile. Fig. 24 illustrates the effect of couple stress parameter C on Sh with respect to slow time. It is depicted from Fig. 24 that with increase in the value of C, the value of Sh also increases. It can also be examined that for low values of C the profiles are nonoscillatory and by increasing C the profiles become oscillatory which shows convection mode. Fig. 25 depicts the effect of frequency of modulation ω on Sh profile. From Fig. 25, we conclude that on increasing ω, the value of Sh remains unaltered whereas the wavelength of oscillation decreases. Figs. 26–31 represent the variation of $A(\tau)$ with respect to slow time and it is observed that the results are qualitatively similar to those of previous cases but the values obtained by $A(\tau)$ are very high as compared to previous cases.

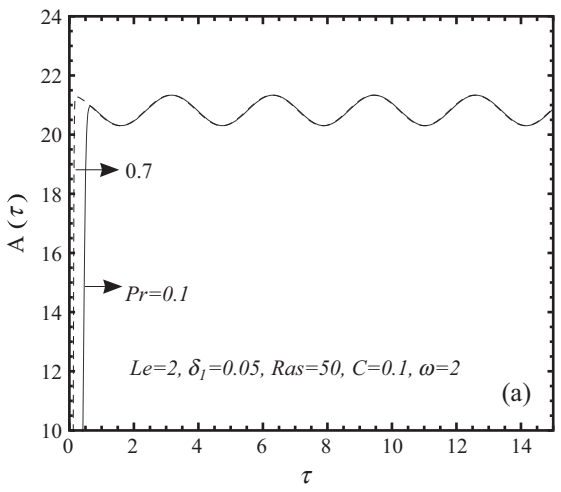

Figure 26 Variation of $A(\tau)$ with time τ for different values of Pr.

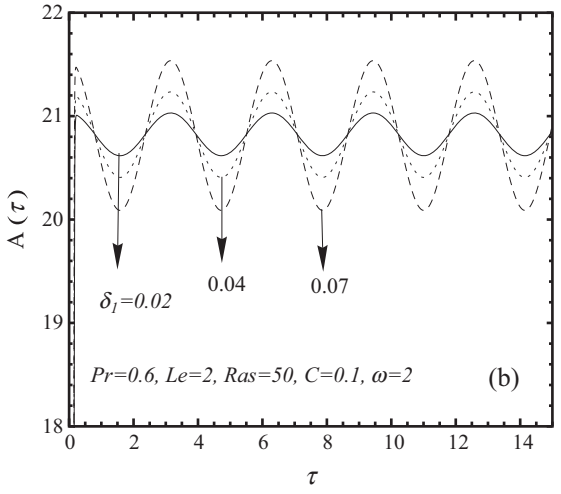

Figure 27 Variation of $A(\tau)$ with time τ for different values of δ_1.

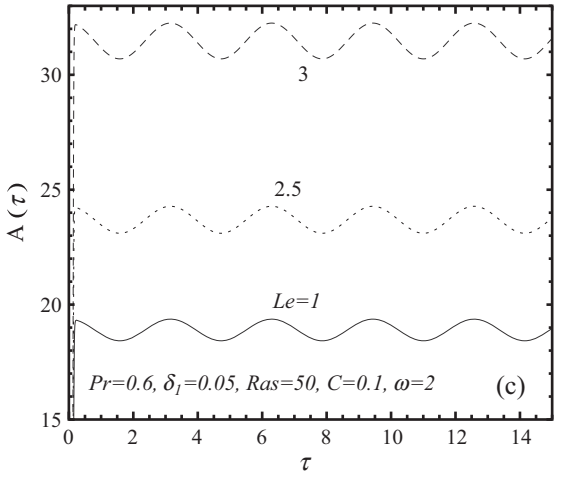

Figure 28 Variation of $A(\tau)$ with time τ for different values of Le.

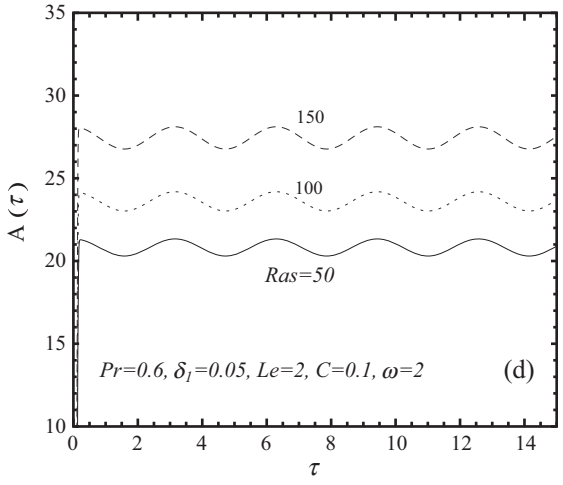

Figure 29 Variation of $A(\tau)$ with time τ for different values of Ra_S.

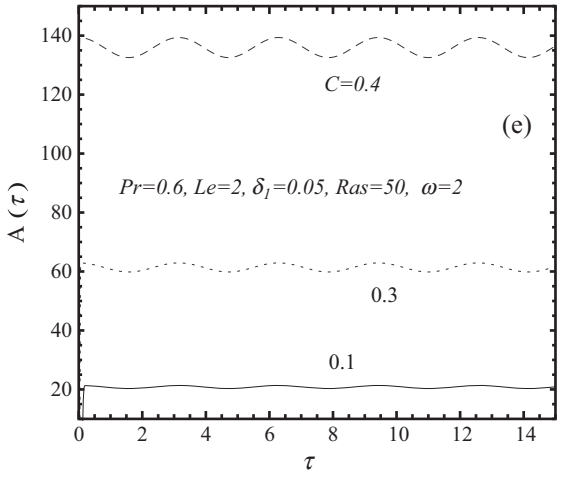

Figure 30 Variation of $A(\tau)$ with time τ for different values of C.

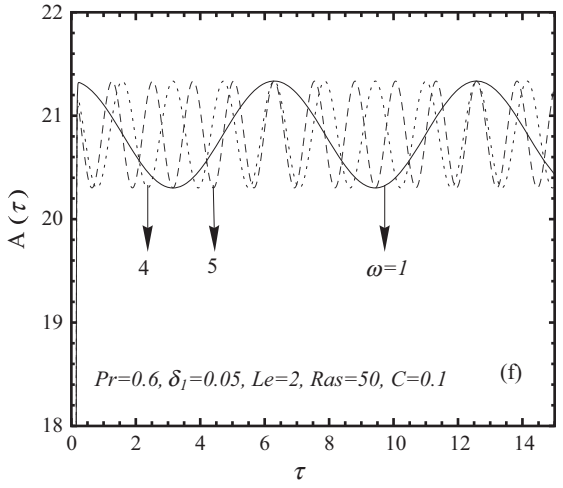

Figure 31 Variation of $A(\tau)$ with time τ for different values of ω.

6. Conclusion

The effect of gravity modulation in a couple stress liquid has been investigated. The Ginzburg–Landau equations have been used to solve the problem. On the basis of above discussion we reached on following conclusions:

1. The streamlines for all values of τ and C are concentric closed curves.
2. The values of stream function are decreasing from hot wall to cold wall which shows that convection is in progress of converting into conduction.
3. For small values of τ the isotherms are contour shaped which indicates that convection is in progress.
4. As τ is increased the isotherms start losing their evenness indicating that conduction is converting into conduction.
5. The effect of increasing Pr, Ra_S, Le and C on Nu and Sh is to increase the rate of heat and mass transfer.
6. The effect of increasing frequency of oscillation is to decrease the wavelength of oscillation.

References

[1] Stokes VK. Couple stresses in fluids. Phys Fluids 1966;9:1709–16.
[2] Malashetty MS, Shivakumara IS, Kulkarni S. The onset of convection in a couple stress fluid saturated porous layer using a thermal non-equilibrium model. Phys Lett A 2009;373:781–90.
[3] Umavathi JC, Malashetty MS. Oberbeck convection flow of a couple stress fluid through a vertical porous stratum. Int J Non-Linear Mech 1999;34:1037–45.
[4] Shivakumara IS. Onset of convection in a couple-stress fluid-saturated porous medium: effects of non-uniform temperature gradients. Arch Appl Mech 2010;80:949–57.
[5] Sharma RC, Thakur KD. Couple stress fluids heated from below in hydromagnetics. Czech J Phys 2000;50:753–8.
[6] Sharma RC, Sharma M. Effect of suspended particles on couple-stress fluid heated from below in the presence of rotation and magnetic. Indian J Pure Appl Math 2004;35:973–89.
[7] Nield DA. Onset of thermohaline convection in a porous medium. Water Resour Res 1968;4:553–60.
[8] Malashetty MS, Gaikwad SN, Swamy M. An analytical study of linear and non-linear double diffusive convection with Soret effect in couple stress liquids. Int J Thermal Sci 2006;45:897–907.
[9] Malashetty MS, Kollur P. The onset of double diffusive convection in a couple stress fluid saturated anisotropic porous layer. Transp Porous Med 2011;86:435–59.
[10] Venezian G. Effect of modulation on the onset of thermal convection. J Fluid Mech 1969;35(2):243–54.
[11] Rosenblat S, Herbert DM. Low frequency modulation of thermal instability. J Fluid Mech 1970;43:385–98.
[12] Rosenblat S, Tanaka GA. Modulation of thermal convection instability. Phys Fluids 1971;14:1319–22.
[13] Roppo MN, Davis SH, Rosenblat S. Benard convection with time-periodic heating. Phys Fluids 1984;27(4):796–803.
[14] Bhadauria BS, Bhatia PK. Time periodic heating of Rayleigh–Benard convection. Phys Scripta 2002;66:59–65.
[15] Siddheshwar PG, Abraham A. Effect of time-periodic boundary temperatures/ body force on Rayleigh–Bnard convection in a ferromagnetic fluid. Acta Mech 2003;161:131–50.
[16] Bhadauria BS. Thermal modulation of Rayleigh–Benard convection. Z Naturforsch 2002;57:780–6.
[17] Malashetty MS, Siddheshwar PG, Swamy M. Effect of thermal modulation on the onset of convection in a viscoelastic fluid saturated porous layer. Trans Porous Media 2006;62:55–79.

[18] Bhadauria BS, Debnath L. Effects of modulation on Rayleigh–Benard convection. Part I. Int J Math Math Sci 2004;19:991–1001.
[19] Gresho PM, Sani RL. The effects of gravity modulation on the stability of a heated fluid layer. J Fluid Mech 1970;40(4):783–806.
[20] Wadih M, Roux B. Natural convection in a long vertical cylinder under gravity modulation. J Fluid Mech 1988;193:391–415.
[21] Malashetty MS, Begum I. Effect of thermal/gravity modulation on the onset of convection in a Maxwell fluid saturated porous layer. Transp Porous Media 2011;90:889–909.
[22] Kumar A, Bhadauria BS. Thermal instability in a rotating anisotrophic porous layer saturated by a viscoelastic fluid. Int J Non-Linear Mech 2011;46:47–56.
[23] Bhadauria BS, Bhatia PK, Debnath L. Convection in Hele–Shawcell with parametric excitation. Int J Non-Linear Mech 2005;40:475–84.
[24] Gupta Vinod K, Singh AK. Double diffusive reaction convection in viscous fluid layer. Int J Ind Math 2014;6:285–97.
[25] Gupta Vinod K, Singh AK. A study of chaos in an anisotropic porous cavity. Int J Energy Technol 2013;5:1–12.
[26] Gupta Vinod K, Prasad R, Singh AK. Effect of magnetic field on chaos in a couple stress liquid saturated in a porous layer. Int J Energy Technol 2013;5:1–9.
[27] Bhadauria BS, Siddheswar PG, Kumar J, Suthar OP. Weakly nonlinear stability analysis of temperature/gravity modulated stationary Rayleigh–Benard convection in a rotating porous medium. Transp. Porous Media 2012;92:633–47.
[28] Srivastava AK, Bhadauria BS, Gupta VK. Magneto convection in an anisotropic porous layer with Soret effect. Int J Non-linear Mech 2012;47:426–38.
[29] Gupta VK, Bhadauria BS. Double diffusive convection in a couple stress liquid saturated in a porous layer with Soret effect using thermal non-equilibrium model. In: Proceeding of ICMSDPA-2012. p. 89–95.
[30] Bhadauria BS, Siddheswar PG, Singh AK, Gupta Vinod K. A local nonlinear stability analysis of modulated double diffusive stationary convection in a couple stress liquid. J Appl Fluid Mech 2016:1255–64.

Dr. Anand Kumar is presently working as an Assistant Professor at Department of Mathematics, Central University of Rajasthan, Ajmer, India. His area of interest is MHD, boundary layer theory, linear and nonlinear thermal instability and flow formation.

Miss Vanita is a Research Scholar in Department of Mathematics, Central University of Rajasthan, Ajmer, India. Her area of interest is MHD, boundary layer theory, linear and nonlinear thermal instability.

Dr. Vinod Kumar Gupta is presently working as assistant professor at department of mathematics, DIT University, Dehradun, India. His area of interest is nonlinear thermal instability and nonlinear dynamics and chaos.